Lossy metamaterials: No effective medium properties without noise

R. R. A. Syms,[*] O. Sydoruk, and L. Solymar

Optical and Semiconductor Devices Group, Department of Electrical and Electronic Engineering, Imperial College London,
Exhibition Road, London SW7 2AZ, United Kingdom
(Received 22 October 2011; revised manuscript received 5 December 2011; published 30 December 2011)

Lossy metamaterial elements act as sources of Johnson noise, making such materials inherently noisy. A coupled transmission line model capable of describing the effective medium properties, propagation and internal reflections, the internal noise distribution, and the noise factor is developed. Two analyses are provided, a numerical solution with limited physical insight and an approximation based on physical principles, and excellent agreement is obtained. It is shown that the internal noise spectrum is modified as it couples to the electromagnetic wave, and that there can be no change in permeability without an increase in the noise factor. This result implies that metamaterials will require careful evaluation of their noise performance before use in practical devices.

I. INTRODUCTION

Metamaterials containing metallic resonant elements such as split-ring resonators (SRRs) and rods have received considerable attention because of their ability to provide negative values of permittivity and permeability at frequencies up to the optical range, and the exciting potential applications arising therefrom.[1–6] The resonant elements are typically arranged in an array, and a variety of effective medium theories[7–9] and homogenization methods[10–12] have been developed to recover the effective parameters with different unit cells. The simplest arrangement is a one-dimensional (1D) array.[13–15] In this case, the interaction between an electromagnetic (EM) wave and the medium can be represented using a lumped-element model in which the EM wave is represented as an L-C transmission line and the lossy resonant elements as R-L-C circuits.[16,17]

Considerable attention has been paid to conductor resistance, which introduces propagation loss, and to interelement coupling, which allows the propagation of lattice waves (for example, magnetoinductive[18] and electroinductive[19] waves for magnetically and electrically coupled elements, respectively). However, all resistive elements must act as sources of Johnson noise[20–22] with a flat power spectral density. Dielectrics are an alternative source of loss and noise. A typical L-C resonator might comprise an inductor L with series resistance R and a lossy capacitor formed from a material with complex permittivity $\varepsilon = \varepsilon' - j\varepsilon''$. The latter may be represented as a lossless capacitor C together with an equivalent series resistor $\varepsilon''/(\varepsilon'\omega C)$, where $\omega = 2\pi f$ and f is the frequency, which acts as a thermal noise source. Any associated noise will therefore have $1/f$ spectral dependence and be most important at low frequency.[23,24] Assuming a frequency-independent loss tangent, the contributions to resistance and noise from the two components will be equal when $\omega/\omega_0 = Q_0\varepsilon''/\varepsilon'$, where $\omega_0 = 1/\sqrt{LC}$ is the angular resonant frequency and $Q_0 = \omega_0 L/R$ is the quality factor of the inductor. For typical values of $Q_0 = 100$ and $\varepsilon''/\varepsilon' = 10^{-4}$, $\omega/\omega_0 = 0.01$, implying that the inductor will be the dominant noise source near resonance. This conclusion will be invalid with purely dielectric resonators. However, dielectric noise may be treated in the analysis that follows by appropriately modifying the power spectral density of the noise sources. The aspect of noise appears to have been largely ignored in metamaterials and

may have a profound impact on any potential applications that involve signals. For example, a noisy electromagnetic wave incident on a metamaterial slab as shown in Fig. 1(a) would be expected to exit the slab after suffering multiple reflection, attenuation, and addition of further noise. While amplification may be used to overcome loss, it is considerably more difficult to mitigate the effects of noise.

It is well known that noise may also propagate as a wave in distributed electrical circuits.[25–33] Recently, it was shown that the propagation of noise waves in magnetoinductive (MI) arrays alters the power spectral density of the noise quite dramatically,[34] and similar effects have been noted in other types of electrical lattice.[35] However, interaction with an electromagnetic wave was omitted, and the effective medium properties were consequently ignored. Here, we extend the analysis of 1D magnetoinductive systems to include magnetic coupling to an EM wave in a magnetic metamaterial. We provide two models, a detailed numerical model and an analytic approximation, capable of simultaneously predicting the permeability μ_r and the noise performance of a medium with effective magnetic properties. In each case, multiple reflections are included. We show that the models agree in all their essential points, and that the effects are fundamentally linked. There can be no change in magnetic susceptibility caused by resonators formed from resistive elements without an increase in the noise factor, a conclusion that can be directly anticipated from the fluctuation-dissipation theorem.[21,36–38] Here, we focus on the use of conductors to provide a negative value of μ_r. However, similar conclusions are likely to be reached for negative-index media that contain a second source of noise derived from the conductors providing a negative value of the permittivity ε_r.

In Sec. II, we introduce the full model and a method numerical solution for comparison with later approximations. In Sec. III, we calculate the dispersion relations of the isolated and coupled systems. In Sec. IV, we use a perturbation solution to estimate the propagation constant of the electromagnetic wave and the effective permeability of the medium. In Sec. V, we show how the power spectral density of the noise in the coupled resonator system may be found. In Sec. VI, we show how this noise is transferred to the EM wave and estimate the noise factor of a finite array. Conclusions are presented in Sec. VII.
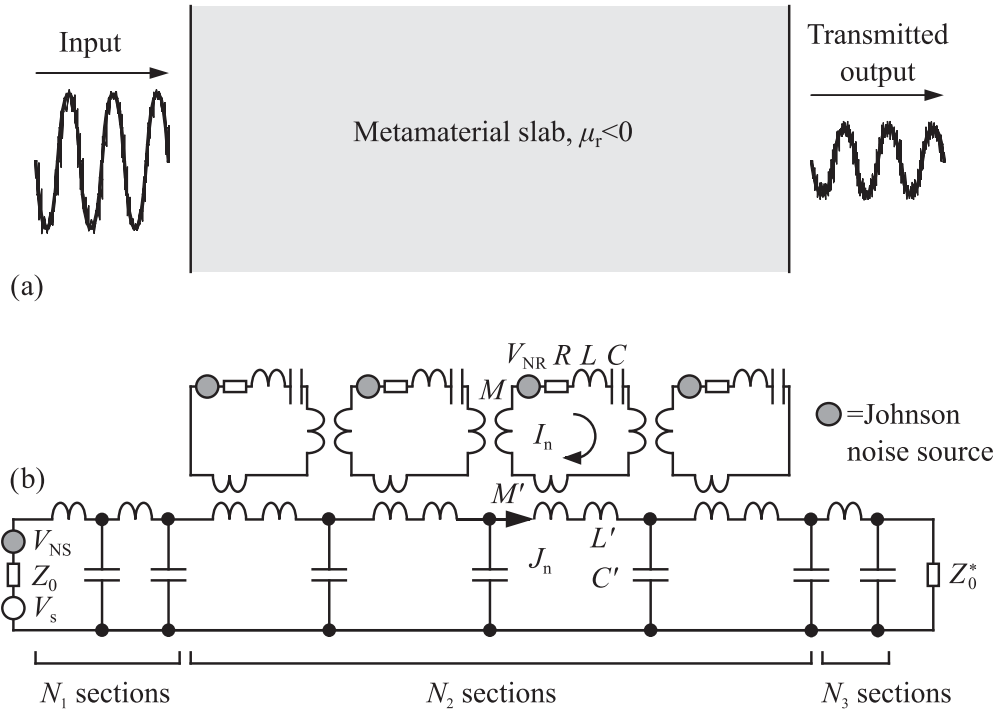
FIG. 1. (a) Accumulation of loss and noise in a RF metamaterial slab; (b) coupled circuit model of an electromagnetic wave interacting magnetically with a chain of lossy resonators.

II. PHYSICAL MODEL

Initial analysis of SRRs largely ignored their electric response.[1] However, it was subsequently shown that there could indeed be an electric response, depending on the internal arrangement of the SRRs and their orientation with respect to the electric field, and that this effect could be significant (see, e.g., Refs. 39–41). Such a response would of course give rise to a change in effective permittivity, and the inclusion of dielectric losses would allow this permittivity to be noisy. Further complications (such as electric coupling between the elements) allow magnetic coupling to the electromagnetic field to give rise to an electric response, and vice versa, and further possibilities for noise. Here, we emphasize that after a decade of active research and a very large number of papers exploring the wide range of possible effects in metamaterial lattices, the link between effective medium properties and noise has been ignored. As a result, although many exciting phenomena such as negative-index materials, epsilon-near-zero materials, and transformation optics have been explored, and applications such as cloaking and electrically small devices have been proposed, there has been no attempt to investigate what may be a significant performance limitation. In the first paper on the subject, there is a strong case to begin with the simplest possible analysis. Such an approach allows a relatively complicated calculation to be presented clearly, without being obscured by the details of multiple couplings. In many cases, magnetic effects are dominant and, furthermore, can be engineered to be so through careful design of the elements and the lattice.[39,42] We therefore restrict ourselves to magnetic coupling between the EM wave and the elements and between the elements themselves. With this assumption,

the effect of the SRRs may be entirely attributed to changes in permeability. The physical model assumed consists of an EM wave propagating in a waveguide past a one-dimensional array of coplanar resonant elements such as SRRs. The EM wave is polarized so that its magnetic field may interact with the resonators, which then provide an effective magnetic medium. Figure 1(b) shows a low-frequency equivalent circuit, which consists of a pair of coupled lines.[16] The resonators are represented as a 1D lattice of lumped-element circuits of period a, with inductance L, capacitance C, and resistance R, coupled to nearest neighbors by mutual inductance M. Such a line supports MI waves. Due to the resistors, each element contains an independent Johnson noise source V_{NR}. The EM wave is represented by a lossless transmission line of the same period, with parameters $L' = \mu_0 a$ and $C' = \varepsilon_0 a$, where μ_0 and ε_0 are the permeability and permittivity of free space, which is terminated with a matched load. The EM wave is derived from a signal voltage source V_S with output resistance Z_0, where Z_0 is the characteristic impedance of the line. Source noise is represented by the Johnson noise source V_{NS}, which is assumed to arise from the source impedance. All noise sources are assumed to have the same temperature. Coupling between the lines is represented by mutual inductance M', which will be negative here. Currents in the nth element of the EM and MI lines are J_n and I_n, respectively. For ease of comparison with standard Johnson noise expressions, all voltages and currents are specified by the root-mean-square (rms) values.

A mathematical model corresponding to Fig. 1(b) may be constructed by using Kirchhoff's voltage law to generate a set of equations relating currents to voltages. We assume N_1

sections of EM transmission line, followed by N_2 sections of interaction region, and finally N_3 sections of transmission line. However, N_1 and N_3 need only be sufficient to allow later extraction of parameters. The total number of sections is therefore $N_4 = N_1 + N_2 + N_3$, and there are $N_5 = N_4 + N_2$ equations to solve. At the input of the EM line, we will have at angular frequency $\omega = 2\pi f$

$$(Z_0 + j\omega L')J_1 + \frac{J_1 - J_2}{j\omega C'} = V_1. \tag{1}$$

Here, V_1 is an input voltage, which might be due either to signal or to source noise. Between the input of the EM line and the interaction region ($1 < n \leqslant N_1$), and between the interaction region and the load ($N_1 + N_2 < n \leqslant N_4$), we have

$$j\omega L'J_n + \frac{J_n - J_{n+1}}{j\omega C'} - \frac{J_{n-1} - J_n}{j\omega C'} = 0. \tag{2}$$

Within the interaction region ($N_1 < n < N_1 + N_2$), we have

$$j\omega L'J_n + \frac{J_n - J_{n+1}}{j\omega C'} - \frac{J_{n-1} - J_n}{j\omega C'} + j\omega M' I_n = 0,$$

$$\left(R + j\omega L + \frac{1}{j\omega C}\right)I_n + j\omega M(I_{n+1} + I_{n-1}) + j\omega M' J_n$$

$$= V_{\text{NR}\,n}. \tag{3}$$

Here, the voltages $V_{\text{NR}\,n}$ are due to Johnson noise in the MI waveguide elements. Finally, at the load, we have

$$Z_0 J_{N_3} - \frac{J_{N_3-1} - J_{N_3}}{j\omega C'} = 0. \tag{4}$$

Equations (1)–(4) can clearly be written in matrix form as $\mathbf{V} = \mathbf{ZI}$, where $\mathbf{Z}$ is an $N_5 \times N_5$ matrix containing impedances and $\mathbf{V}$ and $\mathbf{I}$ are N_5-element column vectors of voltages and currents, respectively. Their solutions can yield a number of results for comparison with later analytic approximations. For example, the effects of each voltage source may be found. Where these generate traveling waves, forward and backward waves may be separated to yield dispersion characteristics for each one, and reflection and transmission coefficients may also be found. In addition, they may be solved repetitively to find the power dissipated in the load when either the voltage V_1 or one of the voltages $V_{\text{NR}\,n}$ is present in isolation. The results can then be scaled to represent either a signal voltage, or a voltage arising from Johnson noise. Once this has been done, addition of powers may be used to find the internal noise or the signal-to-noise ratio (SNR) at the output (which may then be compared with the SNR at the input to find the noise factor F).

III. DISPERSION RELATIONS

In general, the EM wave will encounter a finite line of resonators. However, we start by considering infinite systems. For the transmission line in isolation, and in the absence of any voltage sources, the assumption of traveling-wave solutions to Eq. (2) leads to the dispersion equation

$$1 - \frac{2\omega_0'^2}{\omega^2} + \frac{2\omega_0'^2}{\omega^2} \cos(k_{\text{EM}}a) = 0. \tag{5}$$

Here, $\omega_0' = 1/\sqrt{L'C'}$ and k_{EM} is the propagation constant of the EM wave. This ω-k relation has the well-known sinusoidal variation, providing low-pass propagation up to a maximum angular frequency $2\omega_0'$. At low frequencies, it approximates to the straight-line relation $k_{\text{EM}}a = \omega/\omega_0'$, and leads to the real-valued characteristic impedance $Z_0 = \sqrt{L'/C'} = \sqrt{\mu_0/\varepsilon_0}$.

Similarly, for a chain of resonators in isolation, this approach leads to the dispersion equation for MI waves:[18]

$$1 - \frac{\omega_0^2}{\omega^2} - j\frac{\omega_0}{\omega Q_0} + \kappa \cos(k_{\text{MI}}a) = 0. \tag{6}$$

Here, $\omega_0 = 1/\sqrt{LC}$ is the angular resonant frequency of the elements and $Q_0 = \omega_0 L/R$ is their quality factor, $\kappa = 2M/L$ is the coupling coefficient and k_{MI} is the propagation constant of the MI wave. For negative κ, the waves are backward. In the absence of losses, this ω-k relation provides band-pass propagation over the range $1/\sqrt{1 + |\kappa|} \leqslant \omega/\omega_0 \leqslant 1/\sqrt{1 - |\kappa|}$. Propagation losses are low at mid-band, rising rapidly at the band edges. The effect of a finite Q factor is to allow additional out-of-band propagation, albeit with very high loss.

For the two lines together, Eq. (3) yields the dispersion relation[16]

$$\left[1 - 2\rho^2\frac{\omega_0^2}{\omega^2} + 2\rho^2\frac{\omega_0^2}{\omega^2}\cos(ka)\right]$$

$$\times \left[1 - \frac{\omega_0^2}{\omega^2} - j\frac{\omega_0}{\omega Q_0} + \kappa\cos(ka)\right] - q^2 = 0. \tag{7}$$

Here, $q^2 = M'^2/(LL')$ is the normalized coupling coefficient between the EM and MI waves, and we have also introduced the ratio $\rho = \omega_0'/\omega_0$. The dispersion equation may be solved to yield an ω-k diagram with two branches. The thin lines in Fig. 2(a) show this characteristic for the lossless case, for the example parameters $\kappa = -0.2$, $q^2 = 0.02$, and $\rho = 20$. These results are in full agreement with previous theories, e.g., Ref. 7. The thick lines show the corresponding results obtained for the two uncoupled systems, to which the coupled solutions are asymptotic. In this frequency range, the asymptotes are straight. For the coupled system, there is a gap between the branches near $\omega/\omega_0 = 1/\sqrt{1 + \kappa} = 1.118$; however, the introduction of loss allows propagation in this region.

IV. EFFECTIVE MEDIUM PROPERTIES

Since the effects of the resonators in this restricted model are entirely magnetic, we first note that the relative permeability can be found from the dispersion relation as $\mu_{\text{r}} = (ka/k_{\text{EM}}a)^2$, where ka corresponds to the electromagnetic branch of the coupled system. In general, k is complex and can be written as $k = k' - jk''$. Its frequency dependence may, of course, be found by solving Eq. (7). The data points in Fig. 2(b) show the variation of ω with k' obtained for $\kappa = -0.2$, $Q_0 = 100$, $q^2 = 0.02$, and $\rho = 20$. The result is similar to Fig. 2(a), but the addition of loss has now allowed propagation in the gap. Identical results can be obtained by numerical solution of the circuit equations for a finite array, separation of the currents into different waves, and extraction of the relevant propagation constant.
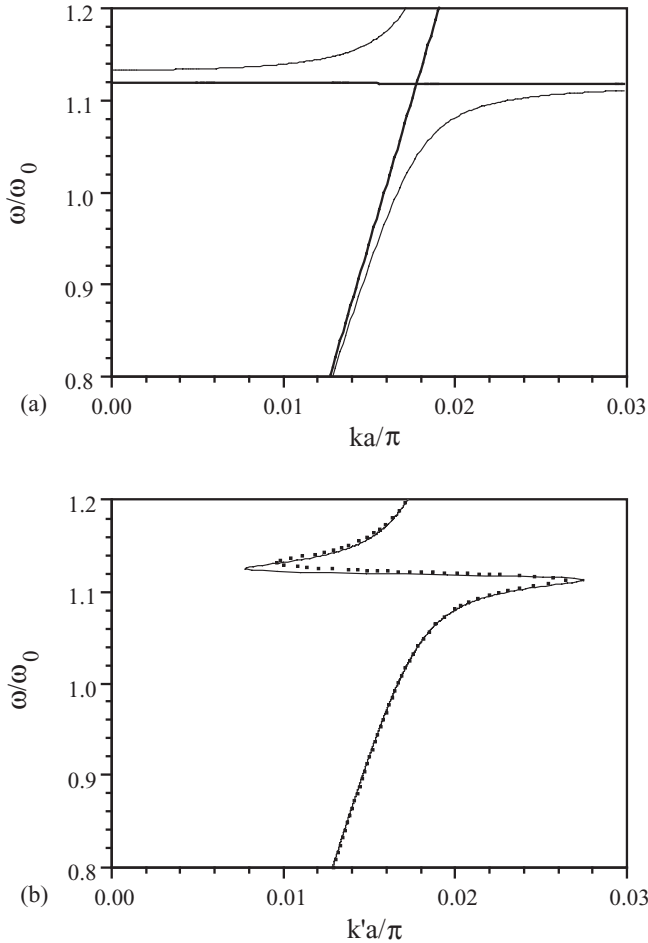
FIG. 2. (a) Dispersion characteristic of lossless coupled system for $\kappa = -0.2$, $q^2 = 0.02$, and $\rho = 20$ (thin lines); corresponding result for uncoupled EM and MI systems (thick lines). (b) Dispersion characteristic of the electromagnetic wave in a lossy coupled system for the parameters above and $Q_0 = 100$. Points: numerical solution; line: approximate solution.
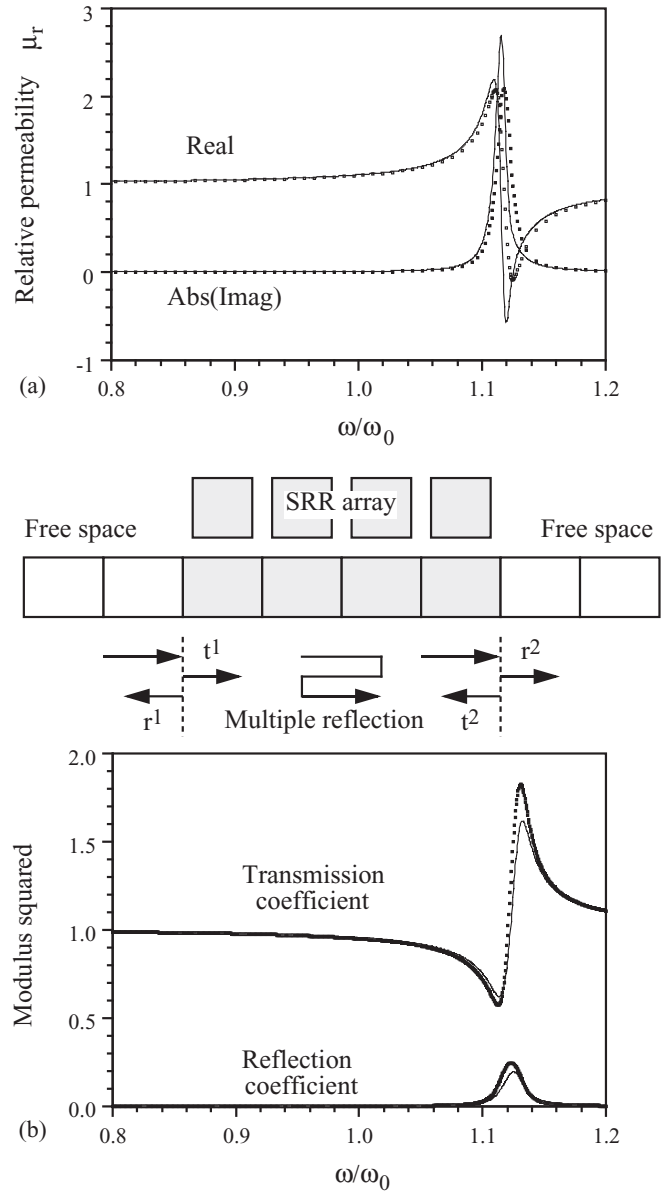

FIG. 3. Frequency variation of (a) the real and imaginary parts of the relative permeability and (b) the transmission and reflection coefficients at the array input for $\kappa = -0.2$, $Q_0 = 100$, $q^2 = 0.02$, and $\rho = 20$. Points: numerical solution; lines: approximate solution.

The data points in Fig. 3(a) show the corresponding frequency variation of the real and imaginary parts of μ_r. The variations show typical resonant behavior, shifted in frequency by the magnetic coupling between the elements to a higher resonant frequency $\omega_0/\sqrt{1+\kappa}$. Although MI wave propagation is supported over a wide band, the effects on the EM wave are restricted to the narrow frequency range where the two are almost synchronous. The real part of the relative permeability can clearly become negative in this region.

Although the numerical value of ka will be used in subsequent calculations, we now present a simple analytic approximation for comparison with published homogenization theories. To do so, we assume that the resonators provide a loading that alters the propagation constant of the EM wave to $k = k_{EM} + \Delta k$. By substituting into Eq. (7), eliminating terms using Eq. (5), neglecting second-order terms, and using the low-frequency approximation for $k_{EM}a$, we obtain

$$ ka = \frac{\omega}{\rho\omega_0} - \frac{q^2\omega}{2\rho\omega_0}\left[\frac{1}{1+\kappa-\omega_0^2/\omega^2-j\omega_0/\omega Q_0}\right]. \quad (8) $$

The full line in Fig. 2(b) shows the variation of ω with k' found in this way for the same parameters as before. There is clearly excellent agreement with the numerical solution. The agreement worsens as Q_0 or q^2 rises since the effect on the EM wave is larger, but for moderate parameters, the perturbation solution provides a very reasonable approximation.

Dividing Eq. (8) by $k_{EM}a$ and squaring the result, we can find the relative permeability as

$$ \mu_r = \left[1 - \frac{q^2/2}{1+\kappa-\omega_0^2/\omega^2-j\omega_0/\omega Q_0}\right]^2. \quad (9) $$

If the interaction term q^2 is small enough, we then get

$$\mu_{\mathrm{r}} = 1 - \frac{q^2}{1 + \kappa - \omega_0^2/\omega^2 - j\omega_0/\omega Q_0}. \tag{10}$$

Equation (10) is clearly identical to expressions commonly found in the literature if q^2 is identified with the so-called filling factor (see Refs. 1 and 2 or the discussion of five separate models for μ_{r} in Sec. 2.8 of Ref. 43). The full lines in Fig. 3(a) show its predictions for the same parameters as before. Once again, there is excellent agreement with the numerical result (the data points).

A change in μ_{r} from unity will of course give rise to reflection at the array boundaries, as shown in Fig. 3(b). Since the model allows a pair of coupled modes, transmission and reflection are both in general accompanied by mode conversion: an electromagnetic wave incident on the array boundary will actually excite not only an EM-like transmitted wave, but also a MI-like wave. Here, for simplicity we ignore the latter, and assume amplitude reflection and transmission coefficients r_1, t_1, r_2, and t_2 for the EM-like wave in standard forms valid for low-frequency current waves incident on a discontinuity between transmission line sections with different magnetic properties

$$r_1 = \frac{k_{\mathrm{EM}} - k}{k_{\mathrm{EM}} + k}, \quad t_1 = \frac{2k_{\mathrm{EM}}}{k_{\mathrm{EM}} + k},$$

$$r_2 = \frac{k - k_{\mathrm{EM}}}{k_{\mathrm{EM}} + k}, \quad t_2 = \frac{2k}{k_{\mathrm{EM}} + k}. \tag{11}$$

The lines in Fig. 3(b) show the frequency dependence of $|r_1|^2$ and $|t_1|^2$ for the same parameters as Fig. 3(a), which shows that these coefficients differ from zero and unity only when the relative permeability also differs significantly from unity. As before, the data points show results obtained from the numerical model. Good agreement is again obtained, with only slight discrepancies where the interaction is at its strongest. Furthermore, examination of the numerical model shows that the MI-like wave is indeed only weakly excited.

V. INTERNAL NOISE

We now consider the internal noise, which arises from Johnson noise in the resonators. If the coupling to the EM wave is weak, little of this noise will be transferred. We therefore begin by considering the resonator array in isolation, assuming this time that it is finite and extends from $n = 1$ to m. For comparison with the full numerical model, we will take $N_2 = m$.

At frequencies low enough for the noise spectrum to be flat, each of the internal noise sources will have rms voltage V_{NR} such that $V_{\mathrm{NR}} V_{\mathrm{NR}}^* = 4KTRdf$ in a small bandwidth df.[20,21] Here, K is Boltzmann's constant and T is absolute temperature. Elsewhere,[34] we have shown that each source in isolation will excite traveling waves, which are reflected at the ends of a finite array as standing noise waves as shown in Fig. 4(a). These waves may then be coupled to the electromagnetic line as shown in Fig. 4(b). However, we will postpone consideration of the more complicated geometry until the following section.
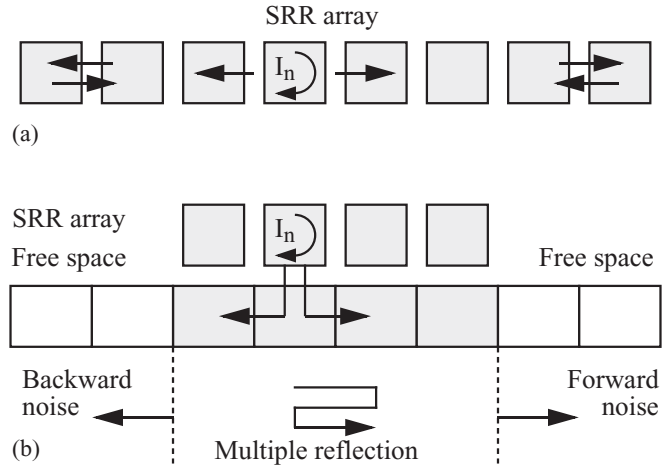

FIG. 4. Model for (a) excitation of noise resonances in a resonator array, and (b) coupling of the array noise to the EM wave.

The driven response of the finite array can be found using a simple theory previously presented for a rather different problem (point excitation in near-field imaging devices[44]). This paper showed how the complete response to excitation of an arbitrary lossy magnetoinductive array could be found as an expansion in terms of the eigenmodes of the same array when lossless and undriven. For the particular case of a regular array with rectangular boundaries, the mode shapes and eigenvalues can be found analytically, allowing calculations to be performed extremely simply. For the 1D array here, the current in the rth element due to a source in the sth element can be found as

$$I_{rs} = \frac{V_{\mathrm{NR}}}{R} \sum_{\nu=1}^{m} \frac{i_{s\nu} i_{r\nu}}{\lambda_\nu}. \tag{12}$$

Here, $i_{s\nu}$ is the normalized shape of the νth resonant mode of the equivalent lossless line, given by

$$i_{s\nu} = \sqrt{\frac{2}{m+1}} \sin\left[\frac{s\nu\pi}{(m+1)}\right] \quad \text{with} \quad \nu = 1, 2, \ldots, m. \tag{13}$$

The term $i_{r\nu}$ is similar, but has s replaced with r. The terms λ_ν are

$$\lambda_\nu = 1 + j\frac{\omega_0}{\omega Q_0}\left(\frac{\omega_0^2}{\omega_\nu^2} - \frac{\omega_0^2}{\omega^2}\right). \tag{14}$$

Here, ω_ν is the angular resonant frequency of the νth eigenmode, given by

$$\omega_\nu^2 = \frac{\omega_0^2}{\sqrt{1 + \kappa \cos[\nu\pi/(m+1)]}}. \tag{15}$$

From Eq. (12), we may obtain

$$I_{rs} I_{rs}^* = \frac{V_{\mathrm{NR}} V_{\mathrm{NR}}^*}{R^2} \left| \sum_{\nu=1}^{m} \frac{i_{s\nu} i_{r\nu}}{\lambda_\nu} \right|^2. \tag{16}$$

Incoherently summing the effect of all noise sources then yields

$$I_r I_r^* R = \frac{V_{\mathrm{NR}} V_{\mathrm{NR}}^*}{R} \sum_{s=1}^{m} \left| \sum_{\nu=1}^{m} \frac{i_{s\nu} i_{r\nu}}{\lambda_\nu} \right|^2. \tag{17}$$
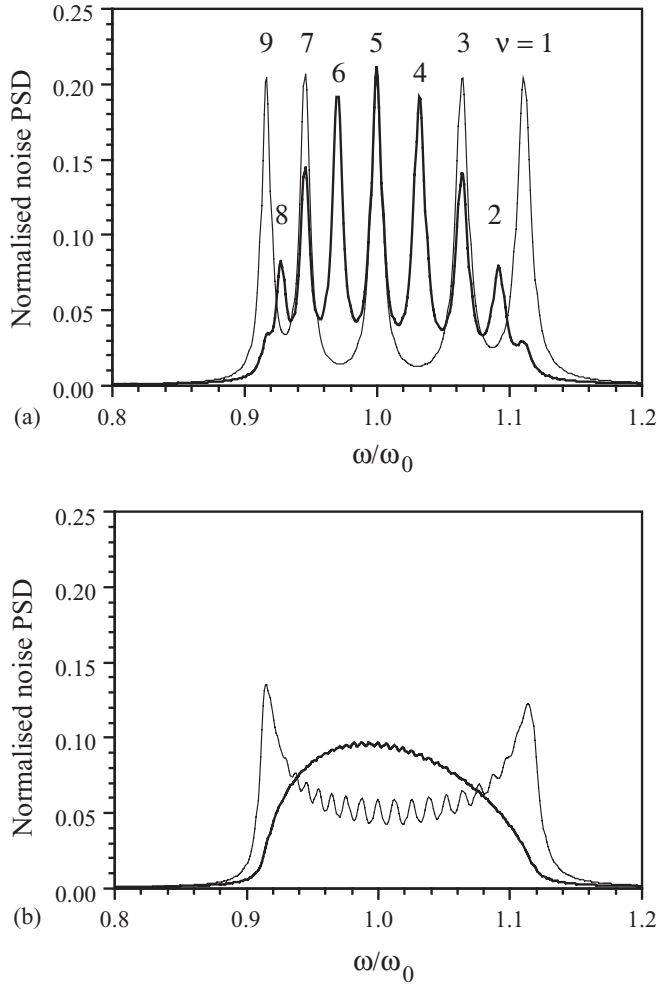
FIG. 5. Frequency variation of the normalized noise PSD for (a) a 9-element and (b) a 49-element resonator array in isolation. In each case, $\kappa = -0.2$ and $Q_0 = 100$, and the thick lines show results for the array edge and the thin lines for the array center.

By using the orthonormality of the modes, we then obtain

$$I_r I_r^* R = \frac{V_{NR} V_{NR}^*}{R} \sum_{\nu=1}^{m} \frac{i_{r\nu}^2}{|\lambda_\nu|^2}. \qquad (18)$$

This result may be written as $I_r I_r^* R = P \times V_{NR} V_{NR}^*/R$. Here, P is a normalized power spectral density (PSD) describing a modification to the otherwise flat spectrum of Johnson noise caused by the reactive elements in the array, given by

$$P(\omega, r) = \sum_{\nu=1}^{m} \frac{i_{r\nu}^2}{|\lambda_\nu|^2}. \qquad (19)$$

This result may be written in full as

$$P = \frac{2}{m+1} \sum_{\nu=1}^{m} \frac{\sin^2[r\nu\pi/(m+1)]}{1 + \left[(Q_0\omega/\omega_0)(\omega_0^2/\omega_\nu^2 - \omega_0^2/\omega^2)\right]^2}. \qquad (20)$$

The PSD was discussed extensively in Ref. 34, and shown to depend on the number of elements m, the position r, the coupling coefficient κ, and the Q factor. Figure 5(a) shows its frequency variation for a nine-element array with $\kappa = -0.2$

and $Q_0 = 100$. The thick and thin lines show results at the array edge ($r = 9$) and center ($r = 5$), respectively. In each case, there is a set of resonances. At the edge, all nine modes are visible. However, only five can be seen at the center since the antisymmetric modes all have zeros at this point and hence make no contribution. Figure 5(b) shows similar results for a 49-element array. Now, the resonances are starting to form a continuum. At the array center, the PSD has assumed a characteristic shape, which tends to the homogeneous result obtained in an infinite array with peaks at the band edges where the propagation losses and modal density are both high. The same results are obtained using the numerical model, if the EM wave is omitted.

VI. NOISE FACTOR

We now consider how the internal noise is coupled to the EM wave. One obvious question is whether the internal noise of the array, which exists over the whole MI band, is transferred to the EM wave unaltered. We also estimate the noise factor F of the array, which is given by

$$F = \frac{S_{in}/N_{in}}{S_{out}/N_{out}}. \qquad (21)$$

Here, S_{in} and N_{in} and S_{out} and N_{out} are the signal and noise powers at the input and output. In a linear device, the noise factor is an intrinsic property and does not depend on the signal power. A key test of the performance of metamaterial devices will be how their attenuation and noise factor compare with those of more conventional solutions.

In addition to the numerical model, we develop an analytic model to explain the physics. Because so many simultaneous equations are involved, construction of such a model is only possible if sweeping approximations are made. Effectively, these amount to assuming weak coupling between the EM wave and the array, so that the perturbations to the propagation constant of the former and the noise distribution of the latter are both relatively small.

Even an approximate model should include reflection at the array boundaries. For example, an incident EM wave should be transmitted at the array input, multiply reflected an infinite number of times, and then transmitted at the output. The amplitude J_m of the current representing the wave at the output of the array may be related to the amplitude J_0 at the input by the sum-of-all-paths method as

$$J_m = J_0 t_1 t_2 e^{-jmka} \left[1 + r_2^2 e^{-2jmka} + r_2^4 e^{-4jmka} \dots \right]. \qquad (22)$$

Summing the exponential terms allows this result to be written as $J_m = t J_0$, where t is an overall amplitude transmission coefficient, given by

$$t = t_1 t_2 \frac{e^{-jmka}}{1 - r_2^2 e^{-2jmka}}. \qquad (23)$$

Clearly, Eq. (23) describes a Fabry-Perot response that allows resonance whenever the round-trip phase change in the array is a whole number of multiples of 2π. However, since the reflection coefficient r_2 is significantly different from unity only at frequencies when there is also loss, high-finesse resonance is unlikely to occur.

As a result of these effects, both the signal and the input noise power alter as they propagate through the array. Hence, we can write

$$S_{\text{out}} = S_{\text{in}}|t|^2,$$
$$N_{\text{out}} = N_{\text{in}}|t|^2 + N_{\text{add}}. \tag{24}$$

Here, N_{add} is the additive noise generated in the resonator array. The noise factor is therefore

$$F = 1 + \frac{N_{\text{add}}}{N_{\text{in}}|t|^2}. \tag{25}$$

For a Johnson noise source at the input, we can immediately write $N_{\text{in}} = KTdf$ for a small bandwidth df.[22] However, to find N_{add}, we must consider how noise is transferred from the resonator array to the EM wave. For weak coupling, a single current I_n in the nth array element will excite a pair of waves into the EM line, traveling in either direction as shown in Fig. 4(b). It is simple to show that the amplitude of each wave is $\kappa_N I_n$, where κ_N is a coupling coefficient given by

$$\kappa_N = -\frac{j}{ka}\frac{M'}{2L'}\left(\frac{\omega}{\rho\omega_0}\right)^2. \tag{26}$$

Excitation of these waves is due to the currents I_{rs} previously given in Eq. (12). If coupling of noise back into the array is neglected, the additive noise is the total power dissipated by all such waves in the load, taking care to account for any coherent effects and multiple reflections. For example, summing all the waves due to a single noise source in the sth resonant element yields an EM current wave leaving the array with total amplitude

$$J_{Ts} = \kappa_N \sum_{r=1}^{m} I_{rs}\left[e^{-j(m-r)ka} + r_2 e^{-j(m+r)ka}\right]t_N. \tag{27}$$

Here, the first exponential describes contributions from all those noise waves that are initially forward going, the second describes all waves that are initially backward going, and t_N is an overall amplitude transmission coefficient that can again be found by the sum-of-all-paths method as

$$t_N = t_2\left(1 + r_2^2 e^{-2jmka} + r_2^4 e^{-4jmka} \dots\right) \tag{28}$$

or as

$$t_N = \frac{t_2}{1 - r_2^2 e^{-2jmka}}. \tag{29}$$

Clearly, the transmission coefficients of the input wave and the additive noise wave are related, as $t_N = (t/t_1)\exp(+jmka)$ and $|t_N|^2 = |t/t_1|^2\exp(2mk''a)$. Consequently, Fabry-Perot resonance will affect both together, and many of the effects will cancel in the final noise factor.

Incoherent addition of the effects of all such noise sources then involves a sum of the form $J_T J_T^* = \sum_{s=1}^{m} J_{Ts} J_{Ts}^*$. Combination with the results of the previous section shows that this can be written as

$$J_T J_T^* = p\frac{\kappa_N \kappa_N^* 4KTdf}{R}|t_N|^2. \tag{30}$$

Here, the function p is given by

$$p(\omega,m) = \sum_{s=1}^{m}\left|\sum_{r=1}^{m}\sum_{v=1}^{m}\frac{i_{sv}i_{rv}}{\lambda_v}(e^{-j(m-r)ka} + r_2 e^{-j(m+r)ka})\right|^2. \tag{31}$$

The additive noise power dissipated in the load may then be found as

$$N_{\text{add}} = J_T J_T^* Z_0. \tag{32}$$

Substitution of Eq. (32) into Eq. (25) shows that the noise factor must be

$$F = 1 + p\frac{4\kappa_N \kappa_N^* Z_0}{R}\frac{e^{2mk''a}}{|t_1|^2}. \tag{33}$$

Minor substitutions then allow this result to be written in the following form:

$$F = 1 + p\frac{q^2}{|ka|^2}\frac{Q_0\omega}{\omega_0}\left(\frac{\omega}{\rho\omega_0}\right)^3\frac{e^{2mk''a}}{|t_1|^2}. \tag{34}$$

The full line in Fig. 6(a) shows the frequency variation of the noise factor obtained using this model for a nine-element array with the same parameters as before ($\kappa = -0.2$, $Q_0 = 100$, $q^2 = 0.02$, and $\rho = 20$). F is close to unity, except at peaks near a discrete set of frequencies that correspond to noise resonances in the magnetoinductive array. Comparison with Fig. 5(a) shows that only odd-order modes can be distinguished, with successively decreasing amplitude. Consequently, the power spectral density of the noise is altered very significantly as it is transferred to the EM wave. The full line in Fig. 6(b) shows corresponding results for a 49-element array. Now, only a single peak may be seen. This peak corresponds to coupling at the frequency at which the effective permeability is most different from unity in Fig. 3(a).

The explanation for this behavior can be found in the form of the function p. For large arrays, the second exponential in Eq. (31) may effectively be disregarded since it will be heavily reduced by attenuation. The summation then represents a phased addition of a single set of terms, and only those adding coherently (which requires the EM and MI waves to be synchronous) will give a significant result. This condition coincides with the condition required for a magnetic effect. Unfortunately, it also corresponds to a frequency range in which the internal noise density at the center of the array is high. Furthermore, both $\mu_r - 1$ (the magnetic susceptibility) and $F - 1$ (the excess noise factor) are proportional to q^2, showing that the two are inescapably linked.

The data points in Figs. 6(a) and 6(b) show the corresponding results from the numerical model. Although there are some small discrepancies in the peak heights, the qualitative agreement is excellent. This result is striking considering the sweeping approximations made in deriving the analytic model, and confirms its essential validity. Effectively, it can provide the same results as a combination of multiple solutions of large numbers of simultaneous equations, and therefore represents a homogenization procedure. For large arrays, the noise factor is determined almost entirely by the propagation constant k and the power transmission coefficient $|t_1|^2$. Here, we have used the numerical value of k, so any discrepancies
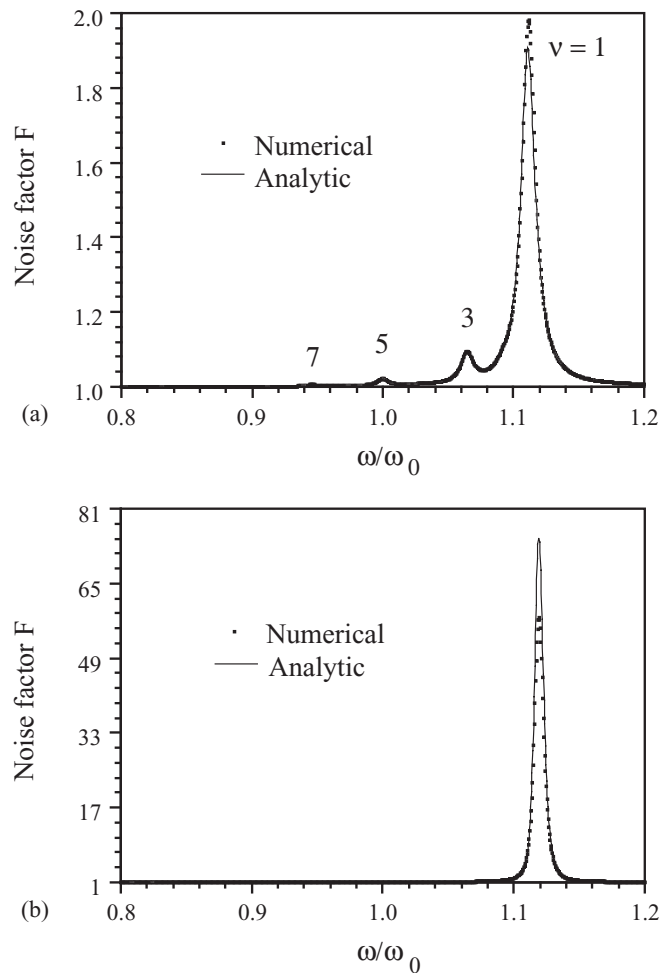
FIG. 6. Frequency variation of noise factor for an electromagnetic wave coupled to (a) a 9-element and (b) a 49-element resonator array. In each case, $\kappa = -0.2$, $Q_0 = 100$, $q^2 = 0.02$, and $\rho = 20$. Points: numerical solution; lines: approximate solution.

are largely due to the errors in the transmission coefficient previously shown in Fig. 3(b). For large m, the analytic model provides a slight overestimate of F; however, both models predict an exponential increase of $F - 1$ with distance as would be expected.

The peak value of F in Fig. 6(a) is approximately 2, corresponding to a noise figure of ≈ 3 dB. Clearly, this result is obtained at the peak of the absorption band, an undesirable operating point. However, the results are clearly considerably worse, and completely unrealistic for device applications, in Fig. 6(b). Better noise figures are clearly obtained off resonance, but in this frequency range, the effect of the medium on the wave is reduced. Further calculations show that the peak attenuation and noise factor increase with Q_0. However, the frequency range over which both are large reduces at the same time, increasing the range of usable performance.

As presented, the expression for the noise factor is relatively clumsy, and further simplifications will certainly be possible. Several terms are slowly varying with frequency, and others tend to simple limits as m rises. However, since thick slabs have high loss, careful thought will have to be given as to how

usable loss and noise performance may be combined with negative parameters.

For a single Johnson noise source, the available noise power (i.e., the power that can be transferred to a matched load) is $P_{av} = KTB$, where B is the bandwidth.[22] At room temperature ($T = 293$ K), we therefore obtain $P_{av} = 4 \times 10^{-14}$ W, 4×10^{-13} W, and 4×10^{-12} W for example bandwidths of $B = 10$ MHz, 100 MHz, and 1 GHz, respectively. These powers are clearly small, and the cumulative effect of many noise sources would be required to obtain a large total noise power. However, it should be emphasized that in any noise factor calculation, one is effectively making comparisons between a relatively small additive noise and a source noise power of similar magnitude.

VII. CONCLUSIONS

We have demonstrated a physical model capable of simultaneously describing the effective magnetic properties and noise of a one-dimensional array of magnetically coupled resonators containing resistive elements. The model shows that any coupling between a resonator array and an electromagnetic wave that gives rise to an alteration in effective permeability also transfers noise to the wave, with a spectral distribution that is related to the power spectral density of the Johnson noise in the array. The transferred noise is concentrated in the frequency range where significant changes in effective permeability occur, so that all such media must be inherently noisy.

We have found a full solution of the model relying on generalized Kirchhoff's equations. Since it is only a numerical solution leading to no physical insight, we have also solved the problem of noise transfer by a set of approximations that render the mathematical problem tractable and offer a clear physical picture. The full solution has been compared with the analytic approximations for the propagation constant, relative permeability, Fresnel coefficients, internal noise distribution, and noise factor, and excellent agreement has been obtained in each case.

The model was chosen to be as simple as possible, subject to the condition that it should yield a realistic description of noise. We have restricted the model to purely magnetic interaction between the EM wave and the metamaterial array, and to purely magnetic interaction between the elements. Future generalizations might involve modification of the equivalent circuit to include modeling of the following:

(i) conducting rods (to model noise in negative-index materials),

(ii) electrical interaction between the EM wave and the elements,

(iii) electrical interaction between the elements,

(iv) non-nearest-neighbor interactions between the elements,

(v) 2D and 3D arrays,

(vi) loss and noise associated with lossy dielectric elements.

Calculations could again be performed directly using a numerical approach, or analytically in terms of noise waves. In each case, care would be required to extract the full range of anisotropic effective medium properties, but many techniques exist for doing so. However, we emphasize that the effects of

any additional noise sources are likely to be cumulative since these are uncorrelated.

Even without these developments, we may draw conclusions about the use of gain. Gain may certainly be used to compensate for attenuation, but only front-end amplification will lead to much improvement in the noise factor because distributed amplification will also amplify any noise due to the medium itself, and, even worse, will create additional noise due to the amplification process. The implications are that all devices designed to exploit negative-index media that contain lossy elements should be critically examined for their noise performance.

---

*r.syms@imperial.ac.uk

[1] J. B. Pendry, A. J. Holden, D. J. Robbins, and W. J. Stewart, IEEE Trans. Microwave Theory Tech. **47**, 2075 (1999).

[2] D. R. Smith, W. J. Padilla, D. C. Vier, S. C. Nemat-Nasser, and S. Schultz, Phys. Rev. Lett. **84**, 4184 (2000).

[3] M. Gokkavas, K. Guven, I. Bulu, K. Aydin, R. S. Penciu, M. Kafesaki, C. M. Soukoulis, and E. Ozbay, Phys. Rev. B **73**, 193103 (2006).

[4] J. Zhou, T. Koschny, M. Kafesaki, E. N. Economou, J. B. Pendry, and C. M. Soukoulis, Phys. Rev. Lett. **95**, 223902 (2005).

[5] V. M. Shalaev, W. Cai, U. K. Chettiar, H.-K. Yuan, A. K. Sarychev, V. P. Drachev, and A. V. Kildishev, Opt. Lett. **30**, 3356 (2005).

[6] G. Dolling, M. Wegener, C. M. Soukoulis, and S. Linden, Opt. Lett. **32**, 53 (2007).

[7] D. R. Smith, D. C. Vier, N. Kroll, and S. Schultz, Appl. Phys. Lett. **77**, 2246 (2000).

[8] T. Koschny, M. Kafesaki, E. N. Economou, and C. M. Soukoulis, Phys. Rev. Lett. **93**, 107402 (2004).

[9] H. Chen, L. Ran, J. Huangfu, T. M. Grzegorczyk, and J. A. Kong, J. Appl. Phys. **100**, 024915 (2006).

[10] D. R. Smith and J. B. Pendry, J. Opt. Soc. Am. B **23**, 391 (2006).

[11] M. G. Silveirinha, Phys. Rev. B **75**, 115104 (2007).

[12] J. D. Baena, L. Jelinek, R. Marques, and M. Silveirinha, Phys. Rev. A **78**, 013842 (2008).

[13] R. Marques, J. Martel, F. Mesa, and F. Medina, Phys. Rev. Lett. **89**, 183901 (2002).

[14] F. Martin, J. Bonache, F. Falcone, M. Sorolla, and R. Marques, Appl. Phys. Lett. **83**, 4652 (2003).

[15] P. A. Belov and C. R. Simovski, Phys. Rev. E **72**, 036618 (2005).

[16] R. R. A. Syms, E. Shamonina, V. Kalinin, and L. Solymar, J. Appl. Phys. **97**, 064909 (2005).

[17] J. D. Baena, J. Bonache, F. Martin, R. Marques, F. Falcone, T. Lopetegi, M. A. G. Laso, J. Garcia-Garcia, M. F. Portillo, and M. Sorolla, IEEE Trans. Microwave Theory Tech. **53**, 1451 (2005).

[18] E. Shamonina, V. A. Kalinin, K. H. Ringhofer, and L. Solymar, Electron. Lett. **38**, 371 (2002).

[19] M. Beruete, M. J. Freire, R. Marques, F. Falcone, and J. D. Baena, Appl. Phys. Lett. **88**, 083503 (2006).

[20] J. B. Johnson, Phys. Rev. **32**, 87 (1928).

[21] H. Nyquist, Phys. Rev. **32**, 110 (1928).

[22] J. R. Pierce, Proc. IRE **44**, 601 (1956).

[23] N. E. Israeloff and X. Wang, Rev. Sci. Instrum. **68**, 1543 (1997).

[24] T. G. M. Kleinpenning, J. Phys.: Condens. Matter **10**, 4245 (1998).

[25] H. Bauer and H. Rothe, Arch. Elekt. Übertragung **10**, 241 (1956).

[26] H. Rothe and W. Dahlke, Proc. IRE **44**, 811 (1956).

[27] P. Penfield, IRE Trans. Circuit Theory **9**, 83 (1962).

[28] H. Bosma, Ph.D. thesis, Technische Hogeschool Eindhoven, 1967.

[29] R. P. Meys, IEEE Trans. Microwave Theory Tech. **26**, 34 (1976).

[30] R. P. Hecken, IEEE Trans. Microwave Theory Tech. **29**, 997 (1981).

[31] N. G. Kanaglekar, R. E. McIntosh, and W. E. Bryant, IEEE Trans. Microwave Theory Tech. **35**, 112 (1987).

[32] S. Withington, Microwave J. **32**, 169 (1989).

[33] S. W. Wedge, IEEE Micr. Guided Wave Lett. **1**, 117 (1991).

[34] R. R. A. Syms and L. Solymar, J. Appl. Phys. **109**, 124909 (2011).

[35] R. R. A. Syms and L. Solymar, in *Proceedings of the 5th International Congress on Advanced Electromagnetic Materials in Microwaves and Optics* (Barcelona, Spain, 2011).

[36] H. B. Callen and T. A. Welton, Phys. Rev. **83**, 34 (1951).

[37] J. Weber, Phys. Rev. **101**, 1620 (1956).

[38] R. Kubo, Rep. Prog. Phys. **29**, 255 (1966).

[39] R. Marques, F. Medina, and R. Rafii-El-Idrissi, Phys. Rev. B **65**, 144440 (2002).

[40] R. Marques, F. Mesa, J. Martel, and F. Medina, IEEE Trans. Antennas Propag. **51**, 2572 (2003).

[41] D. R. Smith, J. Gollub, J. J. Mock, W. L. Padilla, and D. Schurig, J. Appl. Phys. **100**, 024507 (2006).

[42] J. D. Baena, L. Jelinek, R. Marques, and J. Zehentner, Appl. Phys. Lett. **88**, 134108 (2006).

[43] L. Solymar and E. Shamonina, *Waves in Metamaterials* (Oxford University Press, Oxford, 2009).

[44] R. R. A. Syms, E. Shamonina, and L. Solymar, Metamaterials **5**, 8 (2011).